Available online at ScienceDirect

Nuclear Engineering and Technology

journal homepage: www.elsevier.com/locate/net

Original Article

A Criticality Analysis of the GBC-32 Dry Storage Cask with Hanbit Nuclear Power Plant Unit 3 Fuel Assemblies from the Viewpoint of Burnup Credit

Hyungju Yun, Do-Yeon Kim, Kwangheon Park, and Ser Gi Hong *

Department of Nuclear Engineering, Kyung Hee University, 1732 Deogyeong-daero, Giheung-gu, Yongin-si, Gyeonggi-do 17104, Republic of Korea

ARTICLE INFO

Article history:
Received 2 October 2015
Received in revised form
11 December 2015
Accepted 15 January 2016
Available online 8 February 2016

Keywords:
Axial Burnup Distribution
Burnup Credit
Dry Storage Cask
Monte Carlo N-Particle Transport Code, Version 6
Nuclear Criticality Safety Analysis
SCALE 6.1/STandardized Analysis of Reactivity for Burnup Credit using SCALE

ABSTRACT

Nuclear criticality safety analyses (NCSAs) considering burnup credit were performed for the GBC-32 cask. The used nuclear fuel assemblies (UNFAs) discharged from Hanbit Nuclear Power Plant Unit 3 Cycle 6 were loaded into the cask. Their axial burnup distributions and average discharge burnups were evaluated using the DeCART and Multi-purpose Analyzer for Static and Transient Effects of Reactors (MASTER) codes, and NCSAs were performed using SCALE 6.1/STandardized Analysis of Reactivity for Burnup Credit using SCALE (STARBUCS) and Monte Carlo N-Particle transport code, version 6 (MCNP 6). The axial burnup distributions were determined for 20 UNFAs with various initial enrichments and burnups, which were applied to the criticality analysis for the cask system. The UNFAs for 20- and 30-year cooling times were assumed to be stored in the cask. The criticality analyses indicated that k_{eff} values for UNFAs with nonuniform axial burnup distributions were larger than those with a uniform distribution, that is, the end effects were positive but much smaller than those with the reference distribution. The axial burnup distributions for 20 UNFAs had shapes that were more symmetrical with a less steep gradient in the upper region than the reference ones of the United States Department of Energy. These differences in the axial burnup distributions resulted in a significant reduction in end effects compared with the reference.

1. Introduction

The on-site storage capacity for used nuclear fuel assemblies (UNFAs) generated from nuclear power plants in South Korea is projected to reach its maximum in 2024, including the reracking and on-site transportation of UNFAs. As an alternative to this awkward situation, it is necessary to use a dry storage system to store UNFAs generated from domestic

* *Corresponding author.*
E-mail address: sergihong@khu.ac.kr (S.G. Hong).
http://dx.doi.org/10.1016/j.net.2016.01.011

pressurized water reactors (PWRs); however, implementation of a dry storage system requires an accurate safety analysis of the system from the viewpoint of nuclear criticality. In South Korea, the current nuclear criticality safety analysis (NCSA) of CANada Deuterium Uranium UNFAs for a dry storage cask (DSC) assumes that only fresh NFAs with the maximum enrichment are stored in a DSC for a conservative assumption without consideration of the depletion of fissile nuclides and the generation of neutron-absorbing fission products. A dry storage option for PWR UNFAs has not been allowed because of various uncertainties about their average burnup, axial burnup profile, irradiation history, etc. However, the large conservative assumption leads to a significant increase in the DSCs required. Thus, an application of burnup credit (BUC), which takes credit for the reduction of reactivity resulting from fuel depletion, can increase the capacity of a DSC. However, a BUC application introduces much complexity into an NCSA, such as the need for accurate estimations of isotopic inventories, the burnups of UNFAs, the validation of a criticality evaluation with plutonium nuclides and some fission products, among others. In particular, it is important to apply an optimized and realistic axial burnup distribution to the depletion evaluation of an NCSA to estimate the local isotopic compositions within UNFAs and to accurately quantify the nuclide sources of neutron fission or absorption that have a significant effect on the effective neutron multiplication factor (k_{eff}) in a criticality evaluation. The difference between the k_{eff} values estimated with nonuniform and uniform axial burnup distributions is known as the "end effect" [1], which is given as follows:

$$\text{End effect}\ (\Delta k) = k_{eff}(\text{with nonuniform burnup distribution}) - k_{eff}(\text{with uniform burnup distribution}) \quad (1)$$

In this paper, the NCSAs, in consideration of BUC, were performed with respect to the generic 32 PWR assembly BUC (GBC-32) cask with the UNFAs discharged after Cycle 6 of Hanbit Nuclear Power Plant Unit 3 (HBN #3) using the SCALE 6.1/STandardized Analysis of Reactivity for Burnup Credit using SCALE (STARBUCS) sequence and Monte Carlo N-Particle transport code, version 6 (MCNP 6) code. The axial burnup distributions for the discharged NFAs were evaluated by performing the cycle-by-cycle reload core calculations with the DeCART and Multi-purpose Analyzer for Static and Transient Effects of Reactors (MASTER) codes. The axial burnup distributions were then applied to the SCALE 6.1/STARBUCS sequence in which the depletion calculations in the axial burnup zones were performed to estimate the isotopic compositions that were used to estimate the k_{eff}. In addition, the accuracies of the criticality calculations and the end effects estimated with the KENO V.a of the SCALE 6.1/STARBUCS sequence were assessed through a comparison with the MCNP 6 criticality calculations under the same conditions, such as geometry and isotopic compositions. Finally, the maximum initial uranium enrichments that decrease the estimated k_{eff} to a lesser value than the specified upper subcritical limit (USL) of k_{eff} were found for the cask system with different types of UNFA discharged after Cycle 6 of HBN #3 using the SCALE 6.1/STARBUCS sequence.

2. Materials and methods

An NCSA that implements BUC with respect to a DSC is performed mainly through a two-step process: (1) the determination of isotopic compositions within UNFAs to be loaded into a DSC by a depletion analysis and (2) the determination of the k_{eff} value with respect to the DSC by a criticality analysis [2].

In a depletion analysis, isotopic compositions within UNFAs depend on various factors of fresh NFAs and the reactor operation, such as initial enrichment, average specific powers with operating time, axial burnup distribution, and nuclear reaction cross section. In this work, we first evaluated the axial burnup distributions with respect to the UNFAs discharged at the end of Cycle 6. For this purpose, a typical two-step procedure for the core analysis was performed: (1) a NFA depletion analysis with an advanced lattice code for the few homogenized assembly cross sections and (2) a core depletion analysis with a three-dimensional (3D) nodal diffusion code. The NFA calculations were performed with the DeCART 2D code, which uses the method of characteristics to solve the multigroup neutron transport equation without cell homogenization, the subgroup method for resonance self-shielding treatment, and the Krylov subspace method for the depletion calculations. The DeCART 2D code generates the two group homogenization cross sections that are used in the PROLOG program to generate the table sets of the two group cross sections [3]. Then, these table sets were used in the core analysis using the MASTER code, which is a core analysis code that solves the time-independent 3D multigroup diffusion equation with advanced nodal methods, coupled with the depletion equations or the time-dependent 3D diffusion equation for a transient analysis [4]. To evaluate the axial burnup distributions and the assembly discharge burnups, the cycle-by-cycle reload core calculations from the initial cycle to Cycle 6 were performed with the MASTER code. The result of the MASTER calculation provided the axial burnup distributions of the discharged fuel assemblies with the 20 axial nodes. The axial burnup distributions and average assembly discharge burnup were used in the ORIGEN depletion calculation of the SCALE 6.1/STARBUCS sequence for each axial zone, and the depletion calculation provided the isotopic compositions in each axial zone. Then, the criticality estimations for a DSC were performed by the SCALE 6.1/STARBUCS sequence with the Evaluated Nuclear Data Files, Part B (ENDF/B)-VII 238-group cross-section libraries. The STARBUCS sequence is a multigroup Monte Carlo neutron transport computational tool that assists in performing an NCSA of a DSC in consideration of BUC [5]. STARBUCS automatically generates spatial region-dependent nuclide compositions in UNFAs and calculates k_{eff} values in a 3D Monte Carlo neutron transport calculation for a nuclear criticality evaluation. STARBUCS can also perform iterations on the initial enrichment to determine the initial enrichment below which the PWR UNFAs may be loaded into a cask for a specified burnup and USL. In addition, the accuracies of the multigroup Monte Carlo neutron transport calculations done by the KENO V.a of the SCALE 6.1/STARBUCS sequence were assessed by comparing those obtained with the continuous Monte Carlo neutron transport

Table 1 – Design data for the reactor core of Hanbit Nuclear Power Plant Unit 3.

Parameter	Value
Operating power (MWt)	2,815
Active core height (m)	3.81
Number of assemblies	177
Reference Boron Concentration (ppm)	500
Inlet coolant temperature, Hot Full Power (°C)	296.11
Outlet coolant temperature, Hot Full Power (°C)	312.22

calculations by the MCNP 6 with ENDF/B-VII.0 cross-section libraries for each UNFA discharged after Cycle 6. Finally, the SCALE 6.1/STARBUCS sequence was used to search for the maximum initial uranium enrichment that satisfied the nuclear criticality safety condition under a specified USL of k_{eff} for each NFA.

3. Computations and results

3.1. *Determination of axial burnup distribution for HBN #3*

The determination of the axial burnup profiles with respect to the UNFAs discharged at the end of Cycle 6 of HBN #3 requires detailed NFA design data and reactor operation conditions. HBN #3 is a Korean standard nuclear power plant that has a designed thermal power of 2,815 MWt. The reactor core of HBN #3 is loaded with the PLUS7 16×16 NFA, which consists of 236 fuel rods and five large water holes. The design data for the reactor core of HBN #3 are summarized in Table 1. The reactor core accommodates 177 fuel assemblies and the active core height is 3.81 m. Table 2 shows the detailed design data for each different type of NFA in Cycle 6. The reactor core is loaded with nine types of NFA. The initial uranium enrichment range is between 4.10 wt. % and 4.52 wt. %, and some assemblies include eight or 12 burnable absorber rods of 6.0 wt. % gadolinia content. Fig. 1 shows the configuration of the NFAs loaded in Cycle 6. Fig. 2 shows the arrangement of the NFAs in the reactor quarter core of Cycle 6 and the index of each NFA, where the blue, gray, and red regions denote the G-, H-, and J-type NFAs, respectively.

Fig. 3 shows the normalized axial burnup distributions for the reference and 20 UNFAs discharged after Cycle 6, where the reference profile, the red dash line, is a representative normalized PWR axial burnup distribution with 18 equally spaced axial regions and an assembly-averaged burnup greater than 30,000 MWD/MTU, as suggested by Wagner and DeHart [6]. The various colored solid lines represent the axial burnup distributions of 20 UNFAs with 20 equally spaced axial regions, where the numbers of the UNFAs indicate the numbers that are used to represent the NFAs in Fig. 2.

Fig. 3 shows that the reference burnup is different from those of the discharged NFAs at the end of Cycle 6. In particular, the reference burnup has slightly higher normalized burnups up to a 300-cm axial position from the bottom, whereas it has significantly lower burnups above 300 cm than the axial burnups for the 20 UNFAs discharged after Cycle 6. This leads to a much less symmetric profile in the reference burnup distribution. Thus, it can be expected that the axial burnup distributions that differ from the reference can lead to different trends in the end effects.

3.2. *Criticality analysis*

The criticality analysis was performed with respect to the GBC-32 cask, into which 32 UNFAs of the same type that are discharged after Cycle 6 were loaded. The GBC-32 cask design was developed to serve as a computational benchmark with the following conditions: (1) the internal dimensions and geometries are representative of typical United States (U.S.) rail-type casks, (2) the canister accommodates 32 PWR UNFAs, and (3) the UNFA cell size is large enough to accommodate all common PWR UNFA designs in the United States of America. The detailed physical specifications of the NFAs and the GBC-32 cask are summarized in Table 3. The average discharge burnups and axial burnup distributions evaluated in Section 3.1 were applied to the criticality analysis by the SCALE 6.1/STARBUCS sequence. In the SCALE 6.1/STARBUCS sequence, the first step is to perform the depletion analysis by ORIGEN using the original "CE 16×16" cross-section library or two modified "CE 16×16" cross-section libraries. The original "CE 16 × 16" cross-section library was prepared without consideration of gadolinia rods, whereas the modified ones, in this work, include consideration of gadolinia rods. The original CE 16 × 16 cross-section library was applied to the G0-and H0-type UNFAs without gadolinia rods, whereas the modified CE 16 × 16 cross-section libraries generated by TRITON were applied to the G1-, H1-, G2-, and H2-type UNFAs with gadolinia

Table 2 – Detailed design data for the NFAs of HBN#3 Cycle 6.

Type	Fuel enrichment (wt. %^{235}U)	Fuel rods/NFA	Burnable absorber rods/NFA	Burnable absorber content (wt. %)	Loaded cycle
G0	4.10	184	0	0.0	6
G1	4.11	176	8	6.0	6
G2	4.12	172	12	6.0	6
H0	4.52	184	0	0.0	6
H1	4.50	176	8	6.0	6
H2	4.50	172	12	6.0	6
J0	4.48	184	0	0.0	6
J1	4.48	176	8	6.0	6
J2	4.48	172	12	6.0	6

NFA, nuclear fuel assembly.

rods in the ORIGEN depletion calculation under the STARBUCS sequence. The second step is to perform multigroup Monte Carlo neutron transport calculations by KENO V.a, and continuous Monte Carlo neutron transport calculations by MCNP 6 to estimate the criticality for the GBC-32 cask. The continuous transport calculations were performed to assess the accuracies of the multigroup transport calculations by KENO V.a. The transport calculations by KENO V.a and MCNP 6 were performed with 238 energy groups and the continuous cross-section libraries of the ENDF/B-VII version, respectively.

Fig. 4 shows the radial cross section of the GBC-32 DSC loaded with the PLUS7 16 × 16 type of 32 UNFAs. The nuclides considered for the application of BUC were the nine major actinides recommended by the U.S. Nuclear Regulatory Commission [8]: U-234, U-235, U-238, Pu-238, Pu-239, Pu-240, Pu-241, Pu-242, and Am-241.

3.3. NCSA using the SCALE 6.1/STARBUCS sequence and MCNP 6 code

The k_{eff} values for the GBC-32 cask system were calculated for each of the 20 UNFAs discharged at the end of Cycle 6. Three cooling times (0 years, 20 years, and 30 years) were considered to show the effect of cooling time on nuclear criticality. The k_{eff} values for the three cooling times calculated by the SCALE 6.1/STARBUCS sequence and MCNP 6 code are shown in Tables 4–6, respectively, where the estimated standard deviations were very small due to enough total neutron histories within the maximum values of 45 pcm for the SCALE 6.1/STARBUCS sequence and 30 pcm for the MCNP 6 code. The k_{eff} values in round brackets are the results obtained with the original CE 16 × 16 cross-section library, whereas the ones obtained with the modified CE 16 × 16 library are given without round brackets. The results show that the use of the modified library gives larger k_{eff} values except for a few cases (e.g., MCNP 6 results for Cases 27 and 49 with 30-year cooling). The effects of the new modified library on k_{eff} range from −135 pcm to 434 pcm in reactivity. The USL for the cask system was set to be 0.9146 based on the bias uncertainties provided in Scaglione et al. [2] and in the report by the U.S. Nuclear Regulatory Commission report [8]: (1) The U.S. Nuclear Regulatory Commission report [8] recommends that the bias uncertainty is $\Delta k_i = 0.0192$ in the isotopic prediction with ENDF/B-VII library data and actinides-only BUC; (2) Scaglione et al. [2]

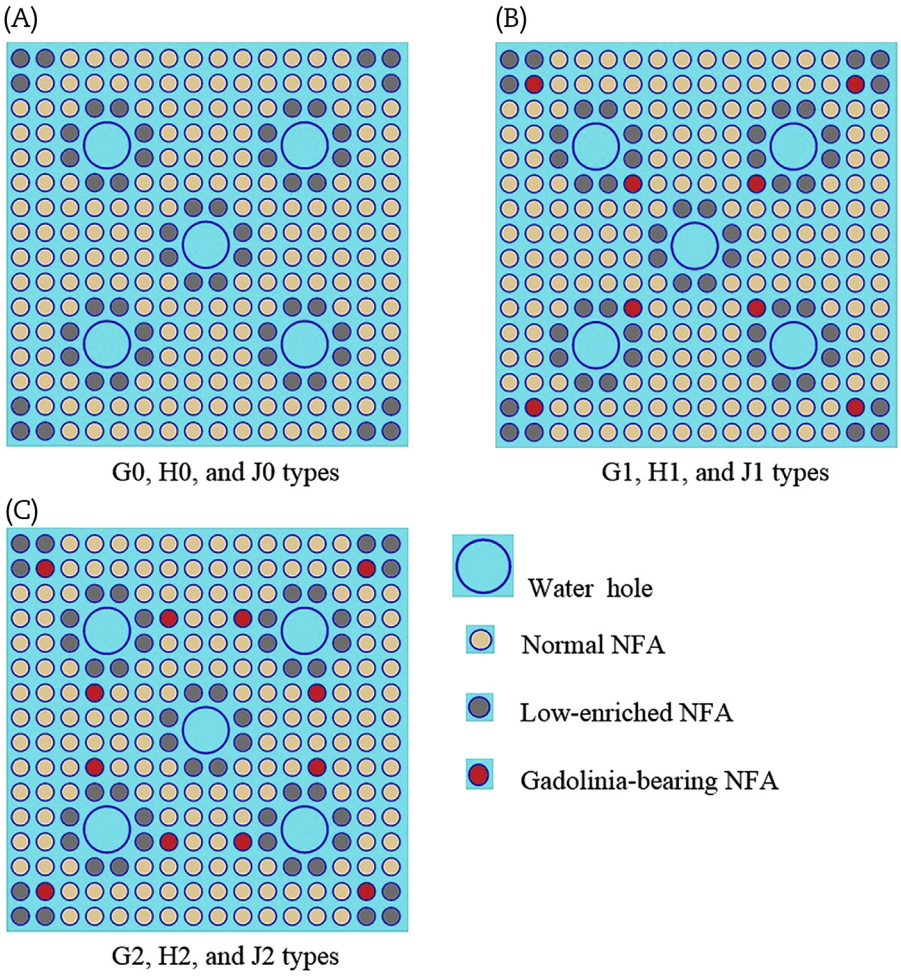

Fig. 1 – Configuration for the nuclear fuel assemblies (NFAs) in Cycle 6 of HBN #3. (A) G0, H0, and J0 types. (B) G1, H1, and J1 types. (C) G2, H2, and J2 types.

G2 1	H1 2	*J2* *3*	H2 4	H0 5	H2 6	*J2* *7*	H2 8
H1 9	*J1* *10*	G2 11	*J1* *12*	G0 13	*J2* *14*	G1 15	*J0* *16*
J2 *17*	G2 18	H2 19	G2 20	H2 21	H1 22	*J1* *23*	G0 24
H2 25	*J1* *26*	G2 27	*J2* *28*	H2 29	H0 30	*J0* *31*	
H0 32	G0 33	H2 34	H2 35	*J2* *36*	H0 37	G2 38	
H2 39	*J2* *40*	H1 41	H0 42	H0 43	*J0* *44*		
J2 45	G1 46	*J1* *47*	*J0* *48*	G2 49			
H2 50	*J0* *51*	G0 52					Type index

Fig. 2 – Arrangement of the nuclear fuel assemblies (NFAs) in the reactor quarter core of Hanbit Nuclear Power Plant Unit 3 Cycle 6 and the index of each NFA.

Table 3 – Design data for the NFA and GBC-32 cask [7].

Parameter	Value (cm)
PLUS7 16X16 NFA data of Hanbit Nuclear Power Plant Unit 3	
Pellet radius	0.41275
Cladding inside/outside radius	0.42256/0.48606
Rod half pitch	0.64410
Guide tube inside/outside radius	1.14495/1.24673
Active fuel/NFA length	381.00/381.96
GBC-32 cask data	
Cell inside/outside radius	11.00/11.75
Cell wall thickness	0.75
Boral panel thickness	0.2565
Boral center thickness	0.2057
Boral Al plate thickness	0.0254
Cell half pitch	11.87825
Boral panel width	19.05
Cell & boral panel height	381.96
Cask inside/outside radius	87.5/107.5
Cask inside/outside height	441.96/501.96
GBC-32 cask boundary condition	
Top & bottom surfaces	Reflecting or mirror condition
X–Y boundaries	Vacuum condition

NFA, nuclear fuel assembly.

recommend that the bias uncertainty is $\Delta k_{\beta} = 0.0162$ in a criticality validation analysis for the actinides-only BUC. The k_{eff} value, 0.9146, of the USL was calculated by subtracting the two bias uncertainties from 0.95, that is, 0.95–0.0192 – 0.0162. These two bias uncertainties were considered to be reasonably conservative values, because the U.S. Nuclear Regulatory Commission report [8] recommends that those are applicable if the SCALE 6.1/TRITON with ENDF/B-VII is used, and it can be justified that this cask system is similar to the GBC-32 cask system.

As shown in Tables 4–6, the UNFAs discharged at Cycle 6 have discharged average burnups that ranged from 31.5 MWD/MTU to 51.9 MWD/MTU. The UNFAs that were not allowed to be stored in the cask having k_{eff} values exceeding 0.9146 are denoted in italic. Table 4 shows that 12 UNFAs, whose indices are 2, 4, 5, 15, 24, 29, 35, 37, 38, 43, 46, and 52 for the cooling time of 0 years, were not allowed to be loaded into the cask because their estimated k_{eff} values exceeded the USL of 0.9146. The high k_{eff} values for these UNFAs were due to their low discharge burnups or high initial uranium enrichments. Tables 5 and 6 show that most of the UNFAs were acceptable to be loaded into the cask for cooling times of 20 years and 30 years. Only three UNFAs, whose indices are 5, 37, and 43, were not allowed to be loaded into the cask due to their highest initial enrichment of 4.52 wt. % and low discharge

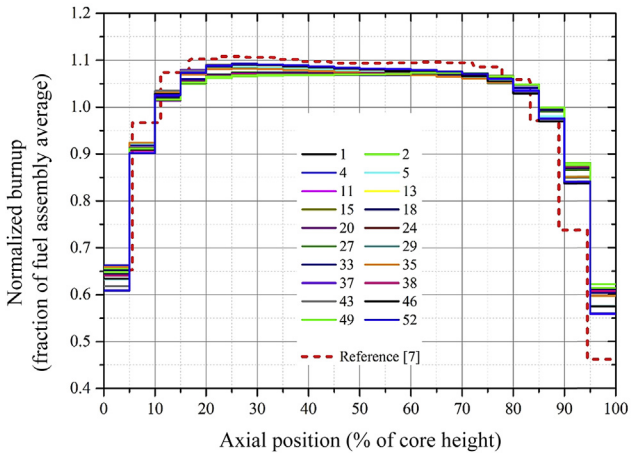

Fig. 3 – Normalized axial burnup distributions for the reference and 20 nuclear fuel assemblies discharged after Hanbit Nuclear Power Plant Unit 3 Cycle 6.

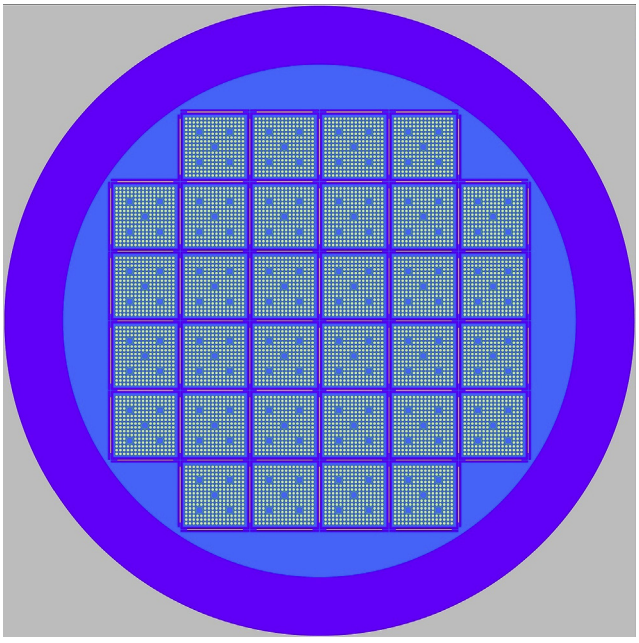

Fig. 4 – Radial cross section of the GBC-32 dry storage cask with 32 used nuclear fuel assemblies.

Table 4 – k_{eff} values for the GBC-32 cask with the UNFAs discharged after Cycle 6 for a 0-year cooling time.[a,b]

Index	Enrichment (wt. %^{235}U)	Burnup (MWD/MTU)	SCALE 6.1/STARBUCS k_{eff}		MCNP 6 k_{eff}	
Axial burnup distribution			Uniform	Nonuniform	Uniform	Nonuniform
1	4.12	51,900	0.86817 (0.86491)	0.86360 (0.86179)	0.86919 (0.86646)	0.86478 (0.86362)
2	4.50	41,060	0.94092	0.93402	0.94141	0.93548
4	4.50	41,120	0.93989	0.93417	0.94178	0.93583
5	4.52	33,920	0.97530	0.96832	0.97651	0.97087
11	4.12	50,130	0.87494 (0.87359)	0.87235 (0.87123)	0.87741 (0.87545)	0.87428 (0.87219)
13	4.10	48,270	0.87971	0.87687	0.88183	0.87931
15	4.11	39,660	0.91856	0.91701	0.92026	0.91847
18	4.12	50,140	0.87510 (0.87256)	0.87151 (0.87050)	0.87740 (0.87493)	0.87409 (0.87208)
20	4.12	42,600	0.90741 (0.90652)	0.90052 (0.90023)	0.90911 (0.90810)	0.90339 (0.90231)
24	4.10	33,160	0.94907	0.94351	0.95106	0.94556
27	4.12	42,580	0.90800 (0.90655)	0.90255 (0.90148)	0.90952 (0.90775)	0.90445 (0.90339)
29	4.50	40,090	0.94504	0.93976	0.94712	0.94223
33	4.10	48,400	0.87944	0.87654	0.88083	0.87925
35	4.50	40,060	0.94411	0.94028	0.94704	0.94245
37	4.52	31,540	0.98514	0.97947	0.98692	0.98248
38	4.12	39,310	0.92313 (0.92113)	0.91582 (0.91539)	0.92399 (0.92322)	0.91807 (0.91765)
43	4.52	31,510	0.98559	0.97969	0.98762	0.98157
46	4.11	39,640	0.91934	0.91661	0.92106	0.91881
49	4.12	41,760	0.91120 (0.91052)	0.90538 (0.90359)	0.91359 (0.91275)	0.90675 (0.90562)
52	4.10	33,170	0.94919	0.94379	0.95043	0.94515

MCNP 6, Monte Carlo N-Particle transport code, version 6; STARBUCS, STandardized Analysis of Reactivity for Burnup Credit using SCALE.
[a] The k_{eff} values in round brackets are the results obtained with the original CE 16 × 16 cross-section library, whereas the ones obtained with the modified CE 16×16 library are given without round brackets.
[b] The UNFAs that were not allowed to be stored in the cask having k_{eff} values exceeding 0.9146 are denoted in italic.

burnups. In Tables 4–6, it should be noted that the KENO V.a and MCNP 6 calculations predicted the same loading allowances of the UNFAs, and the uniform and nonuniform axial burnup distributions also predicted the same loading allowances, even if they produced slightly different k_{eff} values.

The relative discrepancies, in percent mille (pcm), between the k_{eff} values estimated by KENO V.a and MCNP 6 are presented in Table 7. The relative discrepancies between the k_{eff} values calculated by KENO V.a and MCNP 6 were very small within the maximum of 372 pcm, and all the k_{eff} values

Table 5 – k_{eff} values for the GBC-32 cask with the UNFAs discharged after Cycle 6 for the 20-year cooling time.[a,b]

Index	Enrichment (wt. %^{235}U)	Burnup (MWD/MTU)	SCALE 6.1/STARBUCS k_{eff}		MCNP 6 k_{eff}	
Axial burnup distribution			Uniform	Nonuniform	Uniform	Nonuniform
1	4.12	51,900	0.79634 (0.79426)	0.80410 (0.80352)	0.79757 (0.79573)	0.80461 (0.80463)
2	4.50	41,060	0.88933	0.88848	0.88995	0.89081
4	4.50	41,120	0.88803	0.88928	0.89019	0.89034
5	4.52	33,920	0.93490	0.93276	0.93605	0.93529
11	4.12	50,130	0.80649 (0.80437)	0.81640 (0.81478)	0.80772 (0.80569)	0.81636 (0.81580)
13	4.10	48,270	0.81308	0.82207	0.81514	0.82409
15	4.11	39,660	0.86555	0.87443	0.86755	0.87504
18	4.12	50,140	0.80627 (0.80406)	0.81528 (0.81468)	0.80833 (0.80572)	0.81620 (0.81564)
20	4.12	42,600	0.84975 (0.84880)	0.85100 (0.85198)	0.85071 (0.85001)	0.85272 (0.85128)
24	4.10	33,160	0.90621	0.90836	0.90783	0.90867
27	4.12	42,580	0.85024 (0.84873)	0.85365 (0.85267)	0.85068 (0.85024)	0.85547 (0.85389)
29	4.50	40,090	0.89428	0.89789	0.89620	0.90062
33	4.10	48,400	0.81270	0.82185	0.81444	0.82427
35	4.50	40,060	0.89514	0.89844	0.89659	0.90038
37	4.52	31,540	0.94940	0.94685	0.95136	0.94917
38	4.12	39,310	0.86958 (0.86881)	0.86876 (0.86900)	0.87100 (0.87096)	0.87158 (0.87025)
43	4.52	31,510	0.94989	0.94717	0.95150	0.94940
46	4.11	39,640	0.86577	0.87423	0.86716	0.87621
49	4.12	41,760	0.85517 (0.85373)	0.85483 (0.85513)	0.85624 (0.85568)	0.85742 (0.85595)
52	4.10	33,170	0.90614	0.90809	0.90816	0.90947

MCNP 6, Monte Carlo N-Particle transport code, version 6; STARBUCS, STandardized Analysis of Reactivity for Burnup Credit using SCALE.
[a] The k_{eff} values in round brackets are the results obtained with the original CE 16×16 cross-section library, whereas the ones obtained with the modified CE 16×16 library are given without round brackets.
[b] The UNFAs that were not allowed to be stored in the cask having k_{eff} values exceeding 0.9146 are denoted in italic.

Table 6 – k_{eff} values for the GBC-32 cask with the UNFAs discharged after Cycle 6 for a 30-year cooling time.[a,b]

Index	Enrichment (wt. %^{235}U)	Burnup (MWD/MTU)	SCALE 6.1/STARBUCS k_{eff}		MCNP 6 k_{eff}	
Axial burnup distribution			Uniform	Nonuniform	Uniform	Nonuniform
1	4.12	51,900	0.77902 (0.77791)	0.79090 (0.78918)	0.78040 (0.77826)	0.79205 (0.79030)
2	4.50	41,060	0.87729	0.87856	0.87780	0.88069
4	4.50	41,120	0.87627	0.87852	0.87773	0.88118
5	4.52	33,920	0.92514	0.92616	0.92704	0.92719
11	4.12	50,130	0.78939 (0.78811)	0.80264 (0.80199)	0.79146 (0.78925)	0.80412 (0.80390)
13	4.10	48,270	0.79767	0.81064	0.79907	0.81171
15	4.11	39,660	0.85290	0.86462	0.85418	0.86481
18	4.12	50,140	0.78989 (0.78771)	0.80337 (0.80326)	0.79119 (0.78931)	0.80397 (0.80334)
20	4.12	42,600	0.83520 (0.83485)	0.84036 (0.84012)	0.83684 (0.83582)	0.84262 (0.84084)
24	4.10	33,160	0.89661	0.89960	0.89727	0.90140
27	4.12	42,580	0.83667 (0.83503)	0.84412 (0.84122)	0.83743 (0.83603)	0.84420 (0.84476)
29	4.50	40,090	0.88316	0.89016	0.88474	0.88895
33	4.10	48,400	0.79675	0.80983	0.79791	0.81131
35	4.50	40,060	0.88371	0.88999	0.88478	0.89050
37	4.52	31,540	0.94033	0.94075	0.94241	0.94167
38	4.12	39,310	0.85710 (0.85654)	0.86020 (0.85804)	0.85844 (0.85797)	0.86118 (0.86074)
43	4.52	31,510	0.94123	0.94190	0.94252	0.94272
46	4.11	39,640	0.85353	0.86392	0.85438	0.86543
49	4.12	41,760	0.84108 (0.83985)	0.84539 (0.84506)	0.84233 (0.84212)	0.84574 (0.84594)
52	4.10	33,170	0.89667	0.89970	0.89780	0.90064

MCNP 6, Monte Carlo N-Particle transport code, version 6; STARBUCS, STandardized Analysis of Reactivity for Burnup Credit using SCALE.
[a] The k_{eff} values in round brackets are the results obtained with the original CE 16×16 cross-section library, whereas the ones obtained with the modified CE 16×16 library are given without round brackets.
[b] The UNFAs that were not allowed to be stored in the cask having k_{eff} values exceeding 0.9146 are denoted in italic.

calculated by MCNP 6 were larger than those calculated by KENO V.a. Therefore, it can be considered that the NCSA by MCNP 6 was a little more conservative than that by KENO V.a.

The end effects calculated by KENO V.a and MCNP 6 for the three cooling times are shown in Table 8. In addition, the k_{eff} values and the end effects calculated by KENO V.a with the reference burnup distribution for the three cooling times are presented in Table 9. The following observations were made about Tables 8 and 9: (1) all the end effects for the axial burnup distributions of the reference and 20 UNFAs discharged after Cycle 6 became larger as the cooling time increased under the condition of the same initial uranium enrichment, (2) the MCNP 6 code gives similar levels of the end effects to the STARBUCS results, and (3) the end effects estimated with the

Table 7 – Relative discrepancies (pcm) in k_{eff} between KENO V.a and the MCNP 6 code for three cooling times.

Cooling time	0 yr		20 yr		30 yr	
Index	Uniform	Nonuniform	Uniform	Nonuniform	Uniform	Nonuniform
1	135	158	194	79	227	184
2	55	167	78	294	66	275
4	214	190	273	134	190	344
5	127	271	131	290	222	120
11	322	253	189	6	331	229
13	273	316	311	298	220	163
15	201	173	266	80	176	25
18	300	339	316	138	208	93
20	206	353	133	237	235	319
24	220	230	197	38	82	222
27	184	233	61	249	108	11
29	232	279	240	338	202	153
33	179	352	263	357	182	225
35	328	245	181	240	137	64
37	183	313	217	258	235	104
38	101	268	187	372	182	132
43	209	196	178	248	145	92
46	203	261	185	258	117	202
49	287	167	146	353	176	49
52	137	152	245	167	140	116

MCNP 6, Monte Carlo N-Particle transport code, version 6; yr, year.

Table 8 – End effect (pcm) for the cooling times of 0 years, 20 years, and 30 years.

Cooling time	0 yr		20 yr		30 yr	
Index	STARBUCS	MCNP 6	STARBUCS	MCNP 6	STARBUCS	MCNP 6
1	−610	−587	1,212	1,097	1,928	1,885
2	−785	−673	−108	108	165	374
4	−651	−675	158	19	292	446
5	−739	−595	−245	−87	119	17
11	−339	−408	1,505	1,310	2,091	1,989
13	−368	−325	1,345	1,332	2,006	1,949
15	−184	−212	1,173	987	1,589	1,439
18	−471	−432	1,371	1,193	2,124	2,009
20	−843	−696	173	277	735	820
24	−621	−612	261	102	371	511
27	−665	−616	470	658	1,055	958
29	−595	−548	450	548	890	535
33	−376	−204	1,370	1,464	2,027	2,070
35	−431	−514	410	469	798	726
37	−588	−458	−284	−243	47	−83
38	−865	−698	−109	76	420	371
43	−611	−624	−302	−232	76	23
46	−324	−266	1,118	1,191	1,409	1,494
49	−705	−826	−47	161	606	479
52	−603	−588	237	159	376	351

MCNP 6, Monte Carlo N-Particle transport code, version 6; STARBUCS, STandardized Analysis of Reactivity for Burnup Credit using SCALE.

estimated axial burnup distributions of the 20 UNFAs were much smaller than those estimated with the reference axial burnup and the signs of the effects were opposite at a zero cooling time. At a zero cooling time, the negative end effects that were estimated with new axial burnup distributions mean that the criticality calculations with the uniform burnup distribution were more conservative than those with the nonuniform burnup distributions. These analyses revealed that the NCSA with the reference burnup distribution could lead to estimations of the k_{eff} values for the discharged UNFAs from Cycle 6 that were too conservative. In addition, even at longer cooling times, the axial burnup distributions estimated in this work had much smaller end effects than the reference axial burnup distribution, even if they all had the same sign of the end effects except for three UNFAs, that is, those designated by indices 5, 37, and 43.

Therefore, the k_{eff} values and the corresponding end effects for the cask system were significantly dependent on the various

Table 9 – Results of STARBUCS with the reference profile for the cooling times of 0 years, 20 years, and 30 years.

Cooling time	0 yr		20 yr		30 yr	
Index	k_{eff}	End effect (pcm)	k_{eff}	End effect (pcm)	k_{eff}	End effect (pcm)
1	0.89237	3,124	0.84920	7,817	0.83985	9,298
2	0.95222	1,261	0.92023	3,776	0.91434	4,619
4	0.95216	1,371	0.91995	3,907	0.91344	4,644
5	0.97896	383	0.95271	2,000	0.94595	2,378
11	0.89846	2,992	0.85634	7,218	0.84870	8,853
13	0.90229	2,845	0.86256	7,055	0.85396	8,264
15	0.93216	1,588	0.89893	4,290	0.89202	5,142
18	0.89797	2,910	0.85660	7,287	0.84821	8,705
20	0.92270	1,826	0.88679	4,915	0.87903	5,970
24	0.95409	554	0.92673	2,443	0.91965	2,794
27	0.92268	1,752	0.88752	4,940	0.87887	5,739
29	0.95583	1,195	0.92437	3,640	0.91754	4,243
33	0.90195	2,838	0.86158	6,981	0.85339	8,330
35	0.95627	1,347	0.92419	3,512	0.91802	4,229
37	0.98741	233	0.96319	1,508	0.95688	1,839
38	0.93545	1,427	0.90092	4,000	0.89435	4,859
43	0.98694	139	0.96359	1,497	0.95683	1,732
46	0.93193	1,469	0.89832	4,185	0.89175	5,021
49	0.92598	1,752	0.89076	4,672	0.88280	5,619
52	0.95389	519	0.92626	2,397	0.92016	2,847

STARBUCS, STandardized Analysis of Reactivity for Burnup Credit using SCALE.

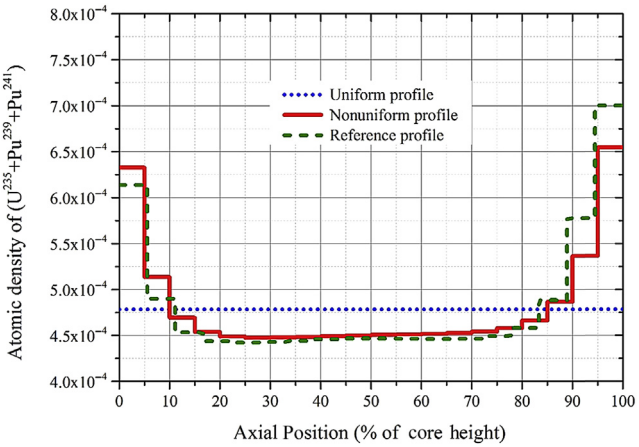

Fig. 5 – Axial distributions of the total atomic density of three fissile nuclides (U^{235}, Pu^{239}, and Pu^{241}) within used nuclear fuel assembly number 52.

axial burnup distributions, as shown in Tables 4–9. To show the effect of the axial burnup distribution on k_{eff}, the axial distributions of three major fissile nuclides' atomic number densities (i.e., U-235, Pu-239, and Pu-241) were analyzed for the different axial burnup distribution cases. For UNFA number 52, as shown in Fig. 5, the total atomic density of these nuclides for the uniform axial burnup distribution was distributed uniformly over the height of the UNFA, but those for the nonuniform and reference axial burnup distributions were shifted toward the axial end of the UNFA, where burnups were relatively low. However, it is known that the axial end regions were more important to the reactivity than the central region in the cask with the UNFAs. Thus, it is considered that the asymmetrical axial burnup distribution having a low burnup in the end region will lead to a larger k_{eff} value. Therefore, it can be expected that the k_{eff} value of the reference axial burnup distribution that had the lowest burnup or largest total atomic density of major fissile nuclides near the axial top was the largest, and the corresponding criticality evaluation was the most conservative. The results for the other 19 UNFAs were similar to those of UNFA number 52.

3.4. *Determination of fuel enrichment to be subcritical for criticality safety*

In the Section 3.3, the upper k_{eff} limit value for the criticality safety of the cask system was set to 0.9146. In this section, the criticality analysis of the cask system was performed by the SCALE 6.1/STARBUCS sequence to search the maximum allowable initial uranium enrichments with the fuel burnup and the axial burnup distributions in Tables 4–6 under the USL. Fig. 6 shows the searched maximum allowable initial uranium enrichments for the UNFAs discharged after Cycle 6. The least-square fitting shows that the initial enrichments became larger linearly as the burnup of the UNFAs increased.

Fig. 6 also shows that the maximum allowable initial uranium enrichments were significantly dependent on the cooling time. That is to say, a longer cooling time led to an increase in the maximum allowable uranium enrichment, mainly due to the decay of Pu-241 and the buildup of Am-241 because of their relatively short half-lives (i.e., 14.35 years and 432.2 years, respectively). In particular, it should be noted that the 20-year cooling time led to a significant increase in the maximum allowable uranium enrichment, whereas the increase of cooling time from 20 years to 30 years led to only a small increase in the maximum allowable uranium enrichment. The axial distributions for the atomic densities of Pu-241 and Am-241 at three cooling times are compared in Figs. 7 and 8, respectively. Fig. 7 shows that the decrease in Pu-241 atomic density due to the 20-year cooling time was significantly greater than that due to the increase in cooling time from 20 years to 30 years. Fig. 8, by contrast, shows that the increase in Am-241 atomic density due to the 20-year cooling time was much greater than that due to the cooling time increase from 20 years to 30 years.

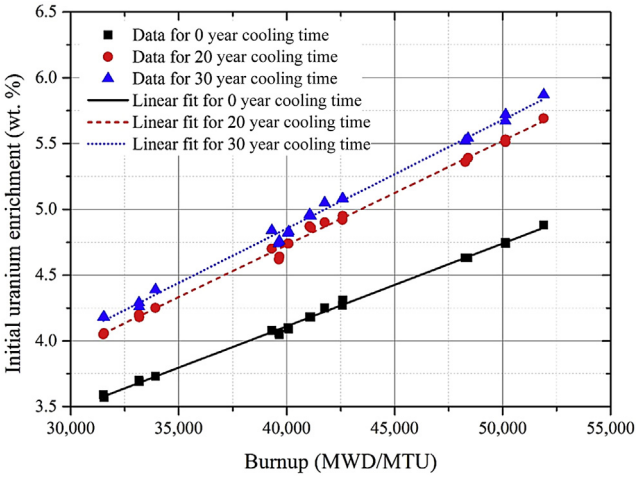

Fig. 6 – Maximum allowable initial enrichments for the used nuclear fuel assemblies discharged after Cycle 6 with cooling time.

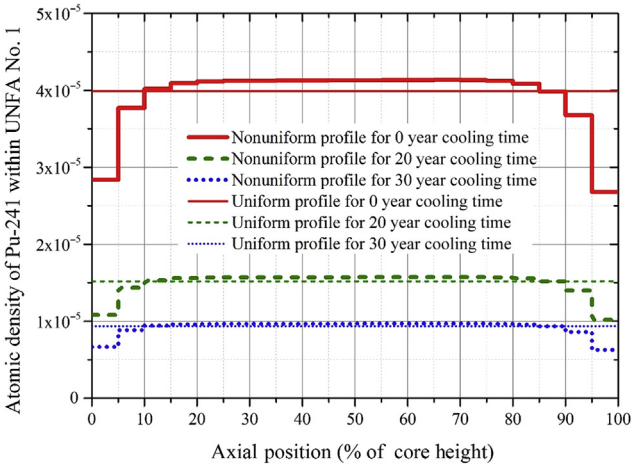

Fig. 7 – Atomic density of Pu-241 within used nuclear fuel assembly (UNFA) number 1 as a function of the cooling time.

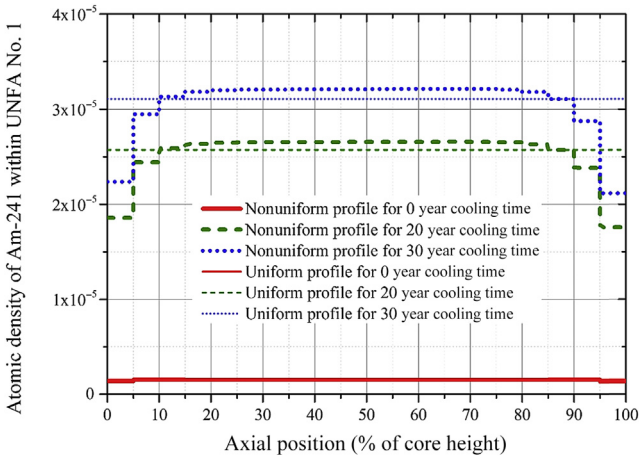

Fig. 8 – Atomic density of Am-241 within used nuclear fuel assembly (UNFA) number 1 as a function of the cooling time.

4. Discussion

In this work, NCSAs in consideration of BUC were performed with respect to the GBC-32 cask within UNFAs discharged after Cycle 6 of HBN #3 by the SCALE 6.1/STARBUCS sequence and the MCNP 6 code. The axial burnup distributions for the UNFAs were evaluated by performing the cycle-by-cycle reload core calculations with the DeCART and MASTER codes. The accuracies of the k_{eff} values and the corresponding end effects for the cooling times of 0 years, 20 years, and 30 years calculated by SCALE 6.1/STARBUCS were assessed through a comparison with the results obtained by MCNP 6. Finally, the maximum allowable initial uranium enrichments under the specified USL for three different cooling times were searched by SCALE 6.1/STARBUCS for each of the UNFAs. From the analysis results, the following was found. (1) Several UNFAs with a low burnup and short cooling time were not allowed to be stored in the GBC-32 cask because their k_{eff} values exceeded the USL, whereas most types of UNFAs after the cooling times of 20 years and 30 years were allowed to be stored in the cask. In particular, the results for the cooling times of 20 years and 30 years should be given more attention than those for the cooling time of 0 years because the UNFAs to be stored in a DSC should actually be stored in a pool storage system for a certain period, which is generally above 20 years after discharge. (2) Most end effects for the cooling times of 20 years and 30 years were positive; in other words, the k_{eff} values for the nonuniform burnup distributions were greater than those for the uniform burnup distribution. Thus, it can be considered that the NCSA by a nonuniform burnup distribution was more conservative than that by a uniform burnup distribution. (3) The axial burnup distributions for the UNFAs discharged from Cycle 6 had slightly different shapes to those suggested by Wagner and DeHart [6]; in particular, in our study, the distributions had more symmetrical shapes with a less steep gradient in the upper region than those reported by Wagner and DeHart [6]. These differences in the axial burnup distributions caused different characteristics of the end effects, that is, much smaller end effects than those with the reference burnup distribution. Therefore, the use of the reference burnup distribution could lead to a conservative result that is too large in the criticality analysis for the UNFAs. (4) The relative discrepancies between the k_{eff} values calculated by KENO V.a and MCNP 6 were very small, within a maximum of 372 pcm, and all of the k_{eff} values calculated using the MCNP 6 code were greater than those calculated using KENO V.a. Therefore, it can be considered that the NCSA by MCNP 6 was a little more conservative than that by KENO V.a. (5) For all the considered UNFAs, MCNP 6 and SCALE 6.1/STARBUCS had very small differences in the end effects. The maximum discrepancy was less than 355 pcm. (6) The total atomic densities of major fissile nuclides at the axial end region played a key role in nuclear criticality, because the axial end region in the cask was more important than the central region. (7) The maximum allowable initial uranium enrichment linearly increased with the discharge burnup. The cooling time of 20 years significantly increased the maximum allowable initial uranium enrichment; however, further cooling did not produce a significant increase in the maximum initial uranium enrichment.

Conflicts of interest

All contributing authors declare no conflicts of interest.

Acknowledgments

This work was supported by the Nuclear Safety Research Program through the Korea Foundation of Nuclear Safety (KOFONS), granted financial resource from the Nuclear Safety and Security Commission (NSSC), Seoul, Republic of Korea (No. 1305032), and by the Space Core Technology Program through the National Research Foundation (NRF), Seoul, Republic of Korea, funded by the Ministry of Science, ICT & Future Planning (No. 2014M1A3A3A02034818). We would also like to thank Doctor Daesik Yook of the Korea Institute of Nuclear Safety, Daejeon, Republic of Korea.

REFERENCES

[1] J.C. Wagner, M.D. DeHart, C.V. Parks, Recommendations for Addressing Axial Burnup in PWR Burnup Credit Analyses, NUREG/CR-6801, ORNL/TM-2001/273, U.S. Nuclear Regulatory Commission, Oak Ridge National Laboratory, Oak Ridge (TN), 2003.

[2] J.M. Scaglione, D.E. Mueller, J.C. Wagner, W.J. Marchall, An Approach for Validating Actinide and Fission Product Burnup Credit Criticality Safety Analyses—Criticality (keff) Predictions, NUREG/CR-7109, ORNL/TM-2011/514, U.S. Nuclear Regulatory Commission, Oak Ridge National Laboratory, Oak Ridge (TN), 2012.

[3] Korea Atomic Energy Research Institute, DeCART 2D v1.0 User's Manual, KAERI/TR-5116/2013, Korea Atomic Energy Research Institute, Daejeon (Korea), 2013.

[4] Korea Atomic Energy Research Institute, MASTER 3.0 User's Manual, KAERI/UM-8/2004, Korea Atomic Energy Research Institute, Daejeon (Korea), 2004.

[5] G. Radulescu, I.C. Gauld, STARBUCS: a Scale Control Module for Automated Criticality Safety Analyses Using Burnup Credit, ORNL/TM-2005/39 Version 6.1, Section C10, Oak Ridge National Laboratory, Oak Ridge (TN), 2011.
[6] J.C. Wagner, M.D. DeHart, Review of Axial Burnup Distribution Considerations for Burnup Credit Calculations, ORNL/TM-1999/246, Oak Ridge National Laboratory, Oak Ridge (TN), 2000.
[7] J.C. Wagner, Computational Benchmark for Estimation of Reactivity Margin from Fission Products and Minor Actinides in PWR Burnup Credit, NUREG/CR-6747, ORNL/TM-2000/306, U.S. Nuclear Regulatory Commission, Oak Ridge National Laboratory, Oak Ridge (TN), 2001.
[8] Division of Spent Fuel Storage and Transportation, Burnup Credit in the Criticality Safety Analyses of PWR Spent Fuel in Transportation and Storage Casks, Interim Staff Guidance (ISG)-8 Revision 3, U.S. Nuclear Regulatory Commission, Washington D.C. (WA), 2012.